Mechanical Systems and Signal Processing (1997) **11**(2), 187–205

ANALYSIS OF COMPUTED ORDER TRACKING

K. R. Fyfe and E. D. S. Munck

Department of Mechanical Engineering, University of Alberta, Edmonton, Alberta, T6G 2G8, Canada

(*Received June* 1995, *accepted June* 1996)

Vibration analysis of rotating machinery is an important part of industrial predictive maintenance programmes, so that wear and defects in moving parts can be discovered and repaired before the machine breaks down, thus reducing operating and maintenance costs. One method of vibration analysis is known as order tracking. This is a frequency analysis method that uses multiples of the running speed (orders), instead of absolute frequencies (Hz), as the frequency base. Order tracking is useful for machine condition monitoring because it can easily identify speed-related vibrations such as shaft defects and bearing wear. To use order tracking analysis, the vibration signal must be sampled at constant increments of shaft angle. Conventional order tracking data acquisition uses special analog hardware to sample at a rate proportional to the shaft speed. A computed order tracking method samples at a constant rate (i.e. uniform Δt), and then uses software to resample the data at constant angular increments. This study examines which factors and assumptions, inherent in this computed order tracking method, have the greatest effect on its accuracy. Both classical and computed methods were evaluated and compared using a digitial simulation. It was found that the method is extremely sensitive to the timing accuracy of the keyphasor pulses and that great improvements in the spectral accuracy were observed when making use of higher-order interpolation functions.

1. INTRODUCTION

In industrial applications, the purpose of rotating machinery analysis is to assess the condition of operating machinery in order to determine what repairs are needed, without shutdown and disassembly of the machine. It should indicate also when this repair should take place. If excessive wear is detected, the machine can be removed from service before it fails. Such analysis can ensure safer operation of machinery by avoiding wear-induced catastrophic failure, and make operating less costly through better management of the repair project. This analysis can be performed in the time, frequency or order domain. Using time domain analysis, one is primarily interested in overall vibration levels. Maximum allowable amplitude levels are determined based on prior experience. Frequency domain analysis reveals the frequency content of the vibration signal. The dominant frequencies are often related to a particular machine component or process in the system and can thus aid in determining the severity of the signal [1, 2]. Order domain analysis relates the vibration signal to the rotating speed of the shaft instead of an absolute frequency base. In this way, vibration components that are proportional to multiples of the running speed can be easily identified.

Order tracking requires sampling of the vibration signal at constant angular increments and hence at a rate proportional to the shaft speed. Classically, this has been accomplished using analog instrumentation to vary the sampling rate proportional to a tachometer

0888–3270/97/020187 + 19 $25.00/0/pg960056

signal; usually a keyphasor pulse [3]. For this procedure, two pieces of specialised equipment are required: a ratio synthesiser and an anti-aliasing tracking filter.

Digital methods have been introduced which resample a constant Δt signal to provide the desired constant $\Delta\theta$ data, based on keyphasor pulses [4–6]. This method is referred to as computed order tracking because it uses numerical techniques to extract speed-normalised data from the vibration signal that has been obtained through traditional sampling methods. The purpose of this paper is to investigate the various factors that affect the accuracy of the computed order tracking method. The primary focus is on how the various assumptions made in using this procedure affect the spectral accuracy and level of the noise floor. Minimisation of the noise floor is important because faint vibration signals need to be identified in the presence of stronger ones rather than having them buried in noise.

1.1. TRADITIONAL MEANS OF ORDER TRACKING

Traditional order tracking directly samples the analog vibration signal at constant shaft increments (i.e. $\Delta\theta$) using analog instrumentation. This normally includes a ratio synthesiser and an anti-aliasing tracking filter. A frequency counter may also be included to monitor the shaft speed. A schematic of this arrangement is shown in Fig. 1.

The ratio synthesiser generates a signal proportional to the shaft speed of the machine. This output is used to control the sampling rate and the cut-off frequency of the analog tracking filter, a low-pass filter with an adjustable cut-off frequency. Once a specified block of data sampled at constant $\Delta\theta$ (angle domain samples) has been obtained, a Fast Fourier Transform (FFT) is calculated resulting in an order spectrum.

The associated cost and complexity of the equipment restrict its use. The analog approach is also prone to error: the equipment used is known to have problems following rapidly changing shaft speeds [7].

1.2. COMPUTED ORDER TRACKING

The computed order tracking method (COT) first records the data at constant Δt increments, using conventional hardware, and then resamples this signal to provide the

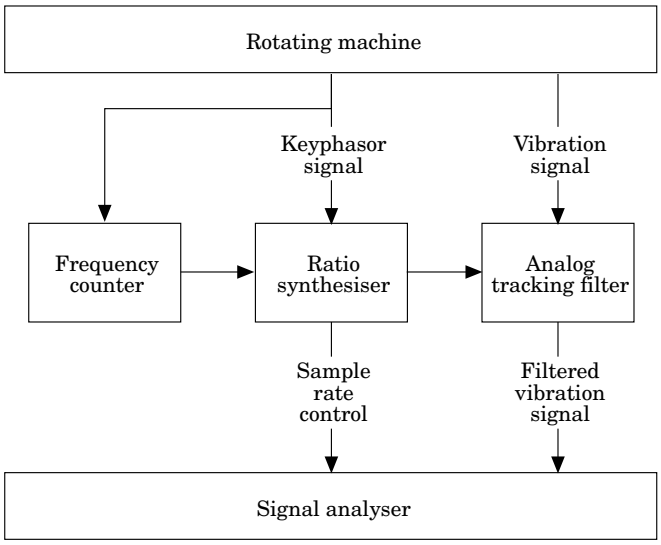

Figure 1. Equipment used for traditional order tracking.

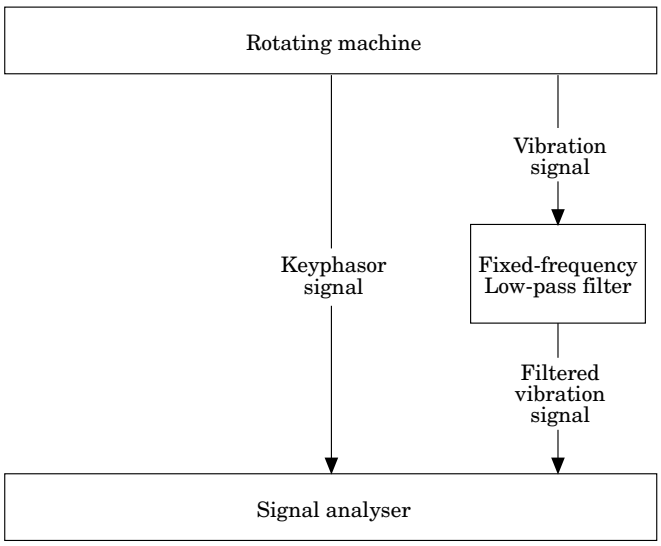

Figure 2. Equipment used for computed order tracking.

desired constant $\Delta\theta$ data, based on a keyphasor signal. This keyphasor signal is typically a once per shaft revolution event that is used to measure the shaft speed and is the reference for measuring the vibration phase angle [8]. In contrast to the traditional method, COT is almost fully digital. Shown in Fig. 2, the vibration signal passes through a fixed frequency low-pass filter, and is sampled at constant increments of time, Δt. To this point, the method resembles traditional frequency analysis more than order tracking. However, once the signal has been sampled, it is resampled by software using the tachometer (or keyphasor) signal to extract signal amplitudes at constant $\Delta\theta$. In Fig. 2, the item labelled signal analyser represents whatever device is used for data acquisition and signal processing. This could be a specialised piece of equipment or a high-speed digital computer with data acquisition hardware.

The analog low-pass filter is often built into the signal analyser or data acquisition system, and is inexpensive. In addition, it typically has better characteristics than its tracking filter counterpart because the design of the latter compromises the effectiveness of the filter at a specific frequency in order to improve its performance over a wide range of frequencies. In contrast, a single-frequency filter can be optimised to perform extremely well at one particular frequency.

Figure 3 illustrates a swept sine signal sampled by a constant increment in the time base (constant Δt). This data must then be resampled at constant increments of shaft angle (constant $\Delta\theta$). The timing of the resample points is based on the duration between available keyphasor pulses. In this example, the resamples are shown at six points per revolution. Note that the resamples fall in the same place on each wave (i.e. peak, trough) independent of where the actual time-based samples were taken.

During resampling, two distinct estimation processes occur. The first involves the correct placement of the resamples on the independent (time) axis. This is the process of sample time determination. Determining the precise resample times is critical for the interpolation process; without precision at this stage, the interpolation process has no hope of consistent accuracy. The second estimation places the resamples on the dependent (amplitude) axis. This is the interpolation process.

To determine the resample times, it will be assumed that the shaft is undergoing constant angular acceleration. With this basis, the shaft angle, θ, can be described by a quadratic equation of the following form:

$$\theta(t) = b_0 + b_1 t + b_2 t^2 \tag{1}$$

The unknown coefficients b_0, b_1 and b_2 are found by fitting three successive keyphasor arrival times (t_1, t_2 and t_3), which occur at known shaft angle increments, $\Delta\Phi$. For example, if there is one keyphasor on the shaft, these increments would occur at intervals of $\Delta\Phi = 2\pi$ radians. This yields the three following conditions,

$$\begin{aligned} \theta(t_1) &= 0 \\ \theta(t_2) &= \Delta\Phi \\ \theta(t_3) &= 2\Delta\Phi \end{aligned} \tag{2}$$

The arrival times, t_1 through t_3 are known from the sampling of the keyphasor pulse signal. Substituting these conditions into equation (1), and arranging in a matrix format gives,

$$\begin{pmatrix} 0 \\ \Delta\Phi \\ 2\Delta\Phi \end{pmatrix} = \begin{bmatrix} 1 & t_1 & t_1^2 \\ 1 & t_2 & t_2^2 \\ 1 & t_3 & t_3^2 \end{bmatrix} \begin{Bmatrix} b_0 \\ b_1 \\ b_2 \end{Bmatrix} \tag{3}$$

This set of equations is then solved for the unknown $\{b_i\}$ components. Once these values are known, equation (1) may be solved for t, yielding

$$t = \frac{1}{2b_2}[\sqrt{4b_2(\theta - b_0) + b_1^2} - b_1] \tag{4}$$

From this equation, any value of θ between 0 and $2\Delta\Phi$ may be entered and the corresponding time, t will be returned. This forms the basis of the resampling algorithm.

The data are resampled after the arrival of each new keyphasor pulse. This most recent keyphasor pulse sets the arrival time of t_3, while the two previous keyphasor arrival times determine t_1 and t_2. To avoid overlap in the sampling, the resample times are calculated

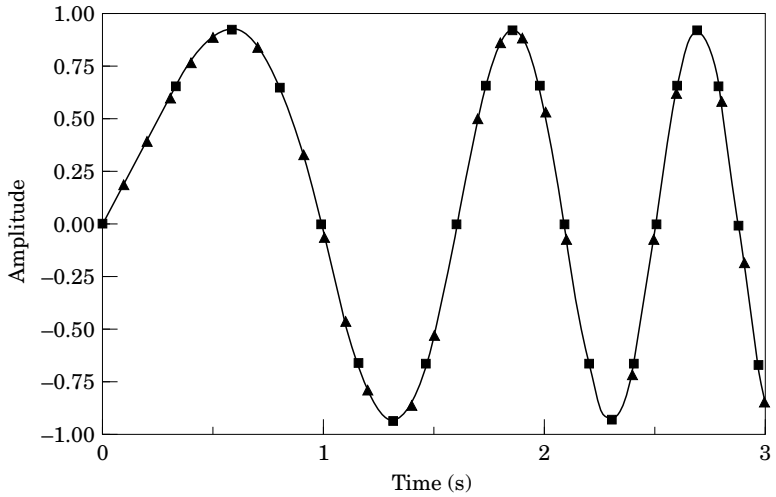

Figure 3. Comparison of data sampling schemes (uniform Δt *vs* uniform $\Delta\theta$). ——, Original data; ▲, uniform Δt; ■, uniform $\Delta\theta$.

only over the center half of the interval ($t_1 \ldots t_3$) [6]. This condition imposes a limit on θ that can be used in equation (4):

$$\frac{\Delta\Phi}{2} \leqslant \theta < \frac{3\Delta\Phi}{2} \tag{5}$$

Normally the resampling of shaft angles is performed discretely such that,

$$\theta = k\Delta\theta \tag{6}$$

where $\Delta\theta$ is the desired angular spacing between resamples. Substituting this expression into equation (5) yields the following values of k (k is a positive integer),

$$\frac{\Delta\Phi}{2\Delta\theta} \leqslant k < \frac{3\Delta\Phi}{2\Delta\theta} \tag{7}$$

So finally, the resampling equation [equation (4)] becomes,

$$t = \frac{1}{2b_2}[\sqrt{4b_2(k\Delta\theta - b_0) + b_1^2} - b_1] \tag{8}$$

See Appendix A for details an an illustrative example on determining resample times.

Once the resample times are calculated, the corresponding amplitudes of the signal are calculated by interpolating between the sampled data using various methods that are discussed in detail in Section 3.5. After the amplitudes are determined, the resampled data are transformed from the angle domain to the order domain by means of an FFT [9], complete with the application of data windows [10].

2. TEST PROCEDURE

A run-up simulation model was programmed to examine various aspects of the computed order tracking method described above [11]. Elements in the simulation include the rotating machine, transducers, amplifier, analog to digital converter, and the processing algorithms. By using a total simulation to test and compare the different methods, it was possible to ensure that only the factors of interest varied from one test to the next. Apparatus for physical experimentation would not be expected to provide such repeatable raw data. An added advantage was the ability to obtain an exact run-up signal in both the time and order domains. This exact signal was used as a base for comparison during the various tests.

For the tests presented in this paper, a resampled data block size of 512 is generated. It is desired to perform an analysis of up to six orders. Thus during the resampling process, 12 samples per revolution are determined. The number of shaft revolutions over which this data is collected is found from: 512 samples $\times$ 1 rev/12 samples = 42.67 revolutions. Thus for each new resampled data block to be generated, it is necessary to collect data from roughly 43 shaft revolutions once a trigger speed is reached. Note that this number is independent of the shaft's starting trigger speed. See Appendix B for more details on the shaft angles and speeds at the beginning and end of the data collection periods.

The simulated vibration signal consists of three sinusoidal components with orders of 1.0, 2.5 and 4.0 containing amplitudes 1.0, 0.5 and 0.5, respectively. The machine is defined to begin at rest and accelerate at a rate of 10 rpm/s with one keyphasor pulse per revolution (except where noted). As the simulation progresses, the vibration and keyphasor signals are being continuously sampled as would be the case if standard analog to digital hardware was used. The simulation tracks the shaft speed by monitoring the time between the

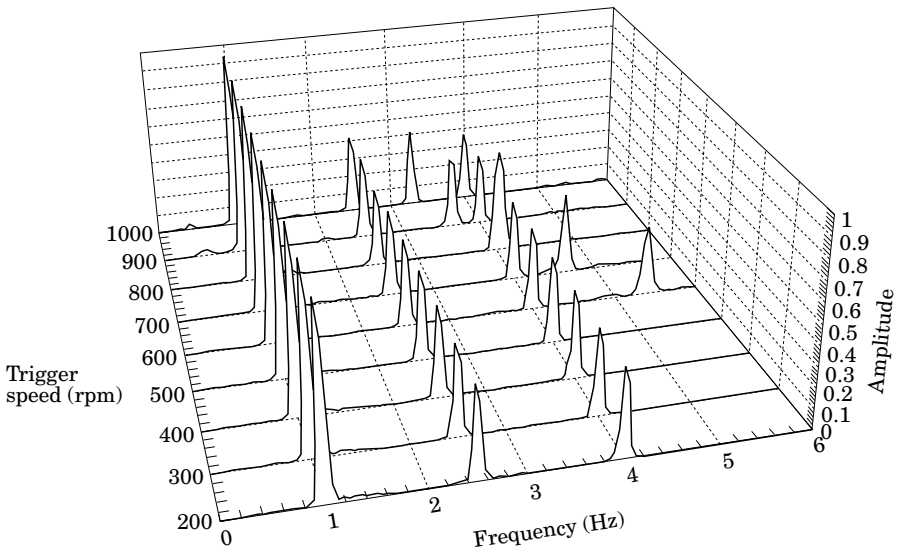

Figure 4. Order digram of simulated machine run-up.

consecutive keyphasor pulses. When the timing between pulses indicates that the shaft speed has reached a trigger speed of 100 rpm, the keyphasor and vibration signals are stored in new buffers. These signals are recorded over the next 43 shaft revolutions (as earlier calculated). These data are stored and analysed during which time the simulation is waiting for the shaft speed to reach the next trigger speed of 200 rpm. This process is continued in 100 rpm increments up to 1000 rpm.

It was necessary to set a sampling rate to avoid aliasing the vibration signal. The highest shaft speed recorded will occur at the end of the 1000-rpm sample block. In testing, the shaft speed at the end of the data block was observed to be no greater than 1050 rpm. In the simulation, it was desired to have an analysis range of up to six orders. Thus, the highest vibration frequency possible in this analysis will be:

$$f_{\max} = 1050 \frac{\text{rev}}{\text{min}} \times \frac{1 \text{ min}}{60 \text{ s}} \times \frac{6 \text{ cycles}}{\text{rev}} = 105 \frac{\text{cycles}}{\text{s}} = 105 \text{ Hz}$$

Nyquist's sampling criteria states that is necessary to sample at greater than twice the highest frequency present in the signal. For this work, a sampling frequency of 250 Hz was selected. A sample run-up of an exact order representation is shown in Fig. 4. In this figure there are three fixed orders at 1.0, 2.5 and 4.0 as well as a fixed frequency component that shows up as a curved path in the upper right-hand side of the figure.

3. ACCURACY OF COMPUTED ORDER TRACKING

Several factors were independently studied to determine their effect on the overall accuracy of the computed order tracking method. These factors include keyphasor timing, use of multiple keyphasors, filtering, rotational speed, interpolation method, noise and block size.

3.1. KEYPHASOR TIMING ACCURACY AND RESOLUTION

The entire method of COT hinges on the accuracy of the resampling process. As was pointed out in the previous section, the resampling process is based on obtaining the times

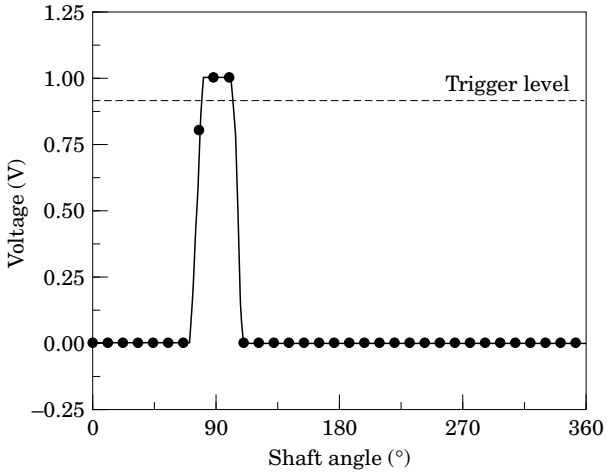

Figure 5. Keyphasor signal: continuous analog signal and discretely sampled counterpart.

at which the keyphasor passes a certain point (i.e. the keyphasor arrival times). The more accurate these times are, the more accurate the resampled data and ensuing spectra. The keyphasor signal, like the vibration signals, is discretely sampled. The rate at which the keyphasor signal is sampled determines the resolution of the keyphasor pulse arrival times. In other words, all keyphasor pulse arrival times will be integer multiples of the keyphasor channel sampling interval, Δt. Figure 5 shows an example of a continuous analog keyphasor signal and its discretely sampled counterpart. It is apparent from this figure that faster sampling rates will result in more accurate keyphasor arrival times (i.e. closer to the set trigger level). This faster sampling helps reduce error, as shown in Fig. 6, where a number of different keyphasor sampling rates are compared. It is seen that an order of

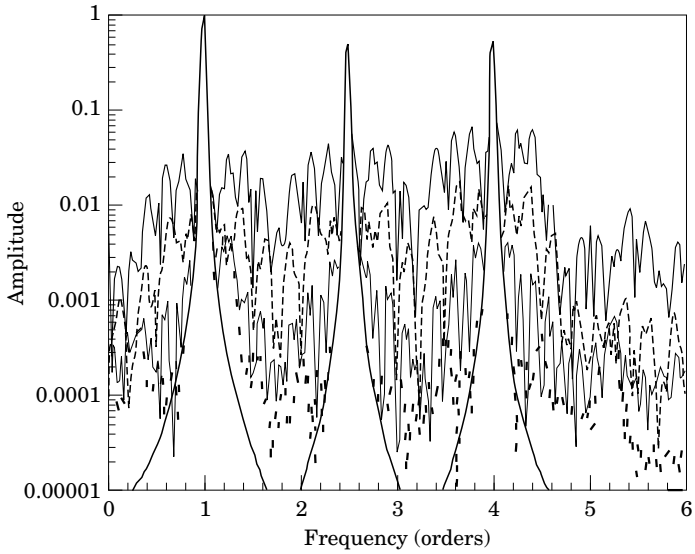

Figure 6. Effects of keyphasor sampling resolution on spectral noise. ——, Exact; —, 250 Hz; – – –, 1 kHz; —, 5 kHz; – –, 50 kHz.

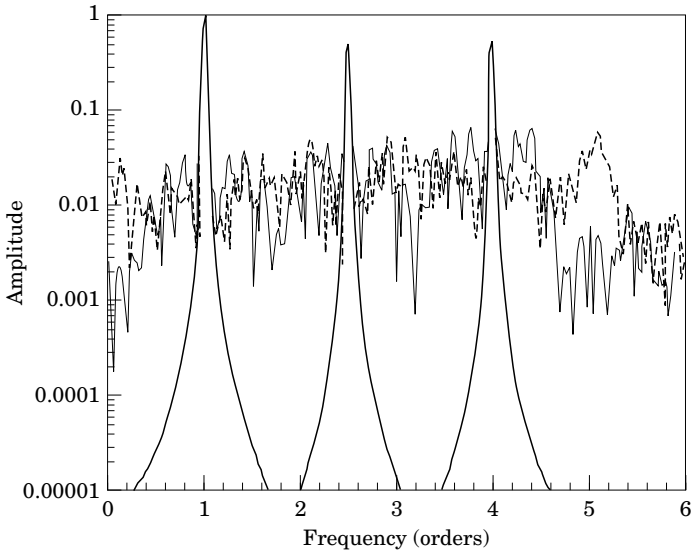

Figure 7. Effect of number of keyphasor pulses at a low sampling rate of 250 Hz. ——, Exact; —, 1 key pulse; – – –, 3 key pulse.

magnitude improvement in the keyphasor sampling resolution produces roughly an order of magnitude improvement in the noise level.

Special note should be made of the lowest keyphasor sampling rate (250 Hz), the same sampling rate used for the vibration signal. Although this is an adequate sampling rate for the vibration signal (i.e. it is above the Nyquist limit), it is very inadequate for the keyphasor signal. If the keyphasor were to be sampled at this low rate, the large multiple side peaks in the spectra would mask any bearing defect frequencies. Common two-channel data acquisition hardware often uses the same sampling rate for both channels. In that case, the choice of sampling rate must be determined by the requirements for keyphasor resolution. Although this increases the data storage requirements, it also greatly improves the interpolation accuracy.

3.2. MULTIPLE KEYPHASOR PULSES PER REVOLUTION

Although utilising one keyphasor per revolution is the most common method, an increased number of keyphasor pulses per revolution may be available. It must be kept in mind, however, that computed order tracking assumes an equal angular separation between keyphasor pulses; if this is not the case in practice, it would cause appreciable errors.

At high sampling rates, single or multiple keyphasors yielded no discernible difference in results. At the low sampling rate of 250 Hz, however, differences in the spectra appeared. This low sampling rate is responsible for the high noise floors present in Fig. 7. In this case, more keyphasor pulses per revolution are not necessarily a good thing. A larger error is present because more keyphasors cause higher distortion in the signal, since any error in the determination of their arrival times is compounded by the more frequent, iterative resampling calculations.

It was anticipated that the use of multiple keyphasors per revolution would improve the results when a highly non-linear run-up acceleration was simlulated since it should now be possible to better track the rapidly changing signal. Despite a large number of trials, test cases were not found to support this argument. It is our conclusion that the arrival

time determination error is dominant, negating any positive effect that might have been obtained with the additional keyphasor information.

3.3. DIGITAL FILTERING

When digitising an analog signal, care must be taken when selecting a sampling frequency to ensure that the sampling rate is at least twice that of the highest frequency present in the signal to prevent aliasing. This minimum sampling rate is known as the Nyquist sampling criteria. Determining this minimum frequency is straightforward if the frequency content of the signal being sampled is known. In general, however, a signal contains information over a broad frequency range and one must apply an analog, low-pass filter before sampling to minimise the effects of aliasing. Typically, the cut-off frequency of the filter will be set at the maximum frequency of interest and the sampling frequency is set at a rate somewhat greater than the minimum sampling rate to minimise the aliasing due to a realistic, non-ideal filter.

The situation is slightly more complicated when considering the resampling of data that has already been sampled at a fixed rate. Consider the test case being modeled: the maximum number of orders of interest is six and the maximum shaft rotation speed is a little over 1000 rpm. This means that the maximum shaft frequency of interest is 6000 rpm and thus the minimum shaft sampling frequency is 12 000 rpm. It is important to remember is that this sampling rate is the same for all rpm that are analysed in the course of a machine run-up (all of the original data acquisition is performed at a constant Δt. If an ideal low-pass filter with a cut-off frequency of 6000 rpm filter is used, any orders over 6000 rpm will be filtered out before the fixed sampling takes place.

Using the above sampling rate and cut-off filter, consider the analysis of a test signal that contains orders of 5.5 and 7. At a shaft speed of 1000 rpm, this would correspond to frequencies of 5500 and 7000 rpm respectively. At this shaft speed, the ideal, fixed frequency, low-pass filter would attenuate the 7000 rpm signal, leaving the 5500 rpm signal intact, which is what is desired. Now consider a slower shaft speed of 100 rpm: the signal still contains orders of 5.5 and 7. Therefore there are frequencies present at 550 rpm and 700 rpm. Now there is a major problem: the analog, fixed-frequency filter (with a cut-off of 6000 rpm) has let the order 7 component slip through! This is a problem because the maximum order of interest is 6, and the order seven component will fold back as if it were order 5! Clearly this is not acceptable. To prevent this, further filtering of the signal must take place. The signal has already been sampled, however, and therefore the signal must be digitally filtered before the resampling process takes place. The cut-off frequencies of these digital filters must change with (or track) the current shaft speed. Thus, the cut-off frequency is dynamic and its value is found by multiplying the cut-off order (in this case: 6) by the machine speed at any point in time. This process of determing a new set of filter coefficients for each shaft speed can be quite CPU intensive, so an interpolated look-up table can be used in its place to significantly speed up the process [11].

3.4. ROTATIONAL SPEED AND ACCELARATION

3.4.1. *Assumption of consistent shaft angle*

Like the vibration signal, the kephasor signal is sampled at constant time intervals. This gives fixed precision in the measurement of the keyphasor pulse arrival times. In the resampling algorithm, a certain shaft angle (0 rad for one keyphasor) is assumed at the keyphasor pulse arrival time. As the machine accelerates, this assumption becomes less valid (Fig. 8). The 1000 rpm signal is deteriorated by this effect with a noise floor almost

one order of magnitude larger than the 400 rpm signal. To explain this, recall that as the keyphasor passes the sensor, it causes a signal to be generated. By the time the acquisition hardware recognises and samples the signal and records an arrival time, the keyphasor has moved to a different angle. Thus, the keyphasor timing precision continually becomes less valid. The result is a decreased accuracy in measuring the keyphasor pulse arrival times. This results in an overall decrease in spectral accuracy at higher rotation speeds.

3.4.2. *Misrepresentation of frequency content*

Generating a spectrum by means of an FFT requires a fixed number of data samples (this study used 512). Obtaining data at constant $\Delta\theta$ increments to obtain these samples requires that the machine execute a fixed number of revolutions, regardless of the trigger speed. If the rotation acceleration is too extreme, the last samples in the set are taken at a significantly different speed from the first ones. Thus, the spectra obtained may not be an accurate snapshot of vibrations present at the trigger speed. Taking this one step further, if the rotation acceleration is even more extreme, the next trigger speed may be reached before enough samples have been obtained for previous trigger speed. This causes problems besides those already mentioned, since if previously used raw data are not stored, the routine cannot go backwards to start from the missed trigger speed. The method could be modified to allow for this occurrence.

3.4.3. *Varying acceleration*

The computed order tracking method assumes a constant acceleration between keyphasor pulses. When this assumption does not hold, the interpolation times are less accurate. This causes two problems. First, the resamples are not taken at constant $\Delta\theta$, so peaks in the spectra may not occur at the right orders. Secondly, when the resample times are in error, the resample amplitudes are inconsistent, causing a higher spectral noise floor.

Because constant acceleration does not occur in the real world, two alterations were made to violate this assumption intentionally. First, a linear acceleration change over the course of a simulated run-up was introduced. However, the resample times are determined

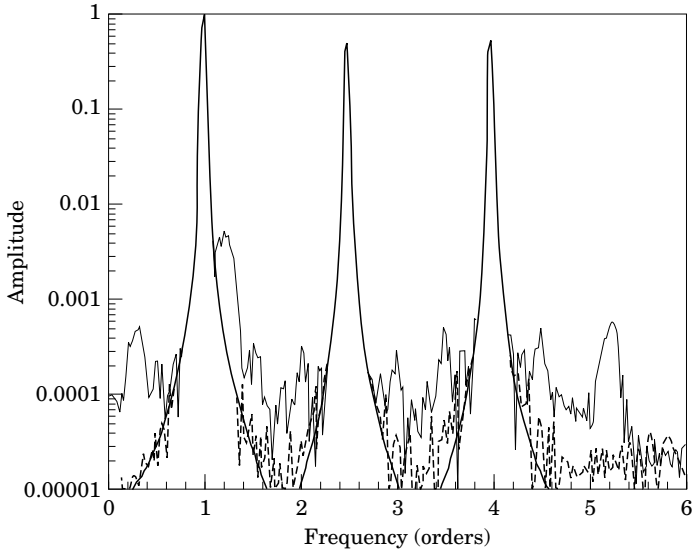

Figure 8. Effect of increased rotation speed on the spectral noise floor. ——, Exact; – – –, 400 rpm; —, 1000 rpm.

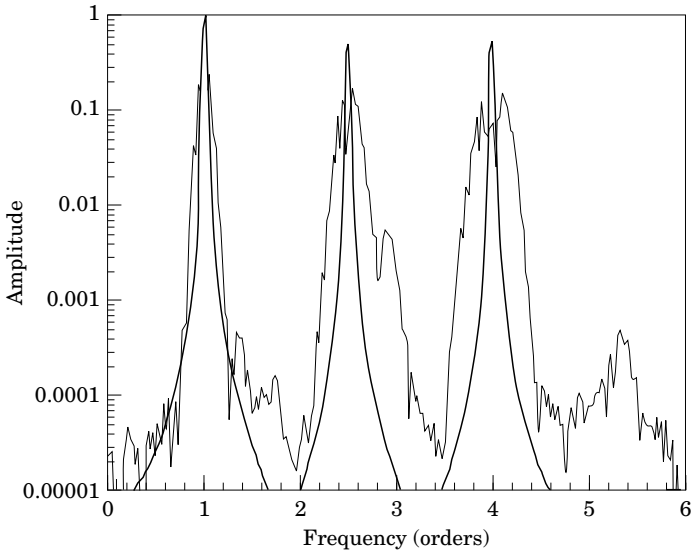

Figure 9. Non-linear acceleration at 1000 rpm. ——, Exact; —, 1000 rpm.

by fitting a quadratic curve to the keyphasor pulse arrival times to obtain a curve of shaft angle *vs* time. Within the time span of three keyphasor pulses, this assumption provides good results even if the acceleration is changing in a linear fashion. With the rate of change kept realistic, the results were virtually unaffected and so are not shown. The second change introduced a moderate sinusoidal fluctuation in the rotation speed, intended to represent a varying acceleration. The spectrum resulting from this non-linear acceleration is shown in Fig. 9 for a shaft speed of 1000 rpm. Notice the wide, irregularly shaped peaks and higher noise floor, all resulting from violation of the constant acceleration assumption. All tests were done with a very fast (50 kHz) keyphasor sample rate. When the keyphasor sample rate is lowered, extreme deterioration of the spectra can be expected, as was discussed in Section 3.1.

At lower rotational speeds, the results are even more dramatic, as shown in Fig. 10 (400 rpm in this case). Because the time interval between successive keyphasor pulses is longer at lower speeds, the same fractional error in the resample times manifests itself as a larger absolute time error, resulting in wider, more irregular peaks. These will hide or imitate bearing defect frequency patterns, especially where smaller sidebands are expected to appear.

3.5. EFFECTS OF INTERPOLATION METHOD

Just as the accuracy of the keyphasor pulse arrival time determines the accuracy of the resample time, the accuracy of the interpolation method determines the accuracy of the resample amplitude. Typically one seeks the most accurate results for the least computational effort. In this study, polynomial interpolation schemes were investigated. It must be remembered that the vibration signals are produced by cyclic phenomena, and are thus sinusoidal, not polynomial. Therefore, these interpolation methods inherently incorporate error into the method. Sinusoidal interpolation approaches were not studied because they require prior knowledge of the signal frequencies.

Three polynomial interpolation methods were examined. The first two, linear and piecewise cubic, fit unique polynomials to the minimum required data points around the

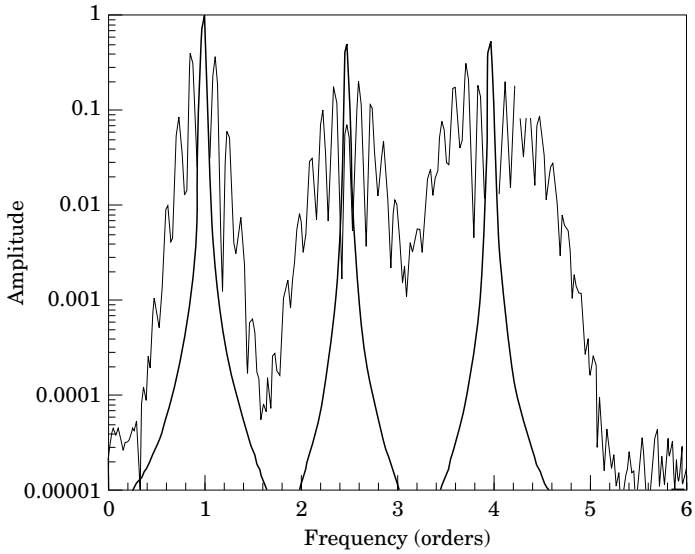

Figure 10. Non-linear acceleration at 400 rpm. ——, Exact; —, 400 rpm.

interpolation point. The third method (blockwise cubic spline) uses all available raw data points in the data set and ensures that the first and second derivatives of the interpolated curve are continuous over the entire data set, thus creating a smooth interpolation curve through the data points.

3.5.1. *Linear interpolation*

An example of simple linear interpolation is shown in Fig. 11. Note the large deviation from the actual signal. When the transducer data are highly oversampled, (e.g. low speeds at the beginning of the run-up) linear interpolation is more accurate. As the sampling rate approaches the Nyquist criterion however, (e.g. high speeds at the end of a run-up)

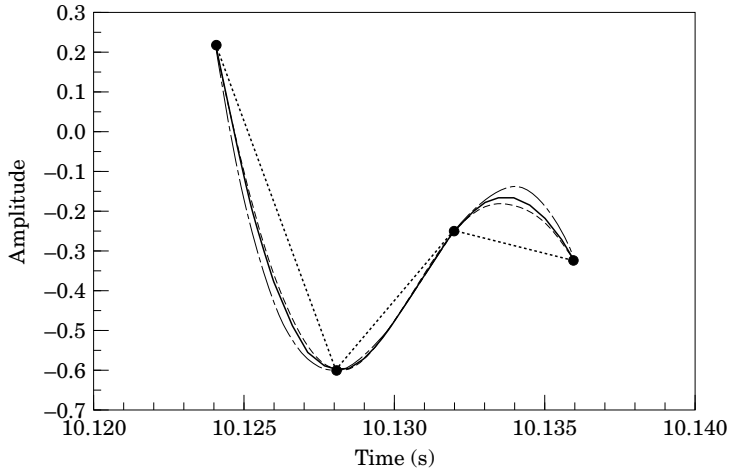

Figure 11. Comparison of interpolation schemes. ——, Exact curve; ···, linear; – — –, cubic polynomial; – – –, spline; ●, sampled data.

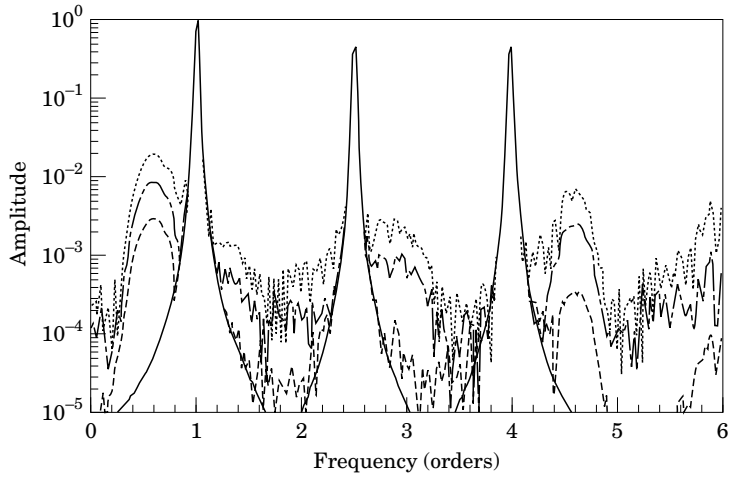

Figure 12. Comparison of spectra of interpolation schemes at 800 Hz. Symbols are as in Fig. 11.

data are not as highly oversampled. In the example illustrated by Fig. 12 (at roughly 800 rpm, near the Nyquist limit), linear interpolation yields a a very high noise floor and large side lobes. Figure 13, on the other hand, displays the same test at 400 rpm with a substantially lower noise floor. Potter [5] recommends using a sampling rate at least twice that suggested by the Nyquist criterion. The sampling rate at 400 rpm meets this recommendation; the sampling rate at 800 rpm does not—it is essentially at the Nyquist limit. In both cases, the simple linear method is inherently noisy.

3.5.2. *Piecewise cubic interpolation*

A significant improvement over linear interpolation comes from using a cubic polynomial. The simplest method of programming cubic interpolation is to use two raw

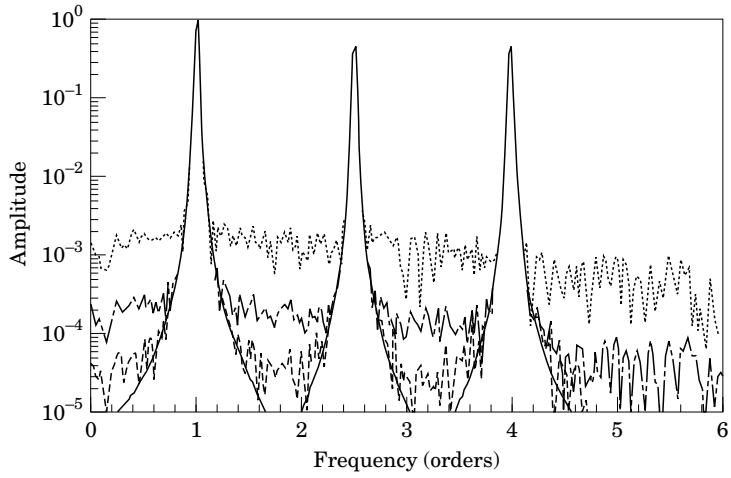

Figure 13. Comparison of spectra of interpolation schemes at 400 Hz. Symbols are as in Fig. 11.

data points before and two points after the interpolation point, fitting a cubic curve to these four points. The equation for the interpolating polynomial is given by,

$$y = a_0 + a_1 t + a_2 t^2 + a_3 t^3 \tag{9}$$

Four sets of data points (i.e. pairs of t_i and y_i) are substituted into equation (9) to generate four independent equations. This system of equations is solved for the coefficients $\{a\}$, which are then used to determine y (the signal amplitude) at any given t (the resample time). Optimised techniques for these calculations are given in [12].

As illustrated in Fig. 11, the application of this cubic polynomial to the same data points as the linear interpolation example yields a curve that is much closer to the original signal. This is also borne out in the frequency domain as shown in Figs 12 and 13; the spectra are much improved over the linear interpolation case.

In performing these calculations, it was found that this piecewise use of the data is extremely sensitive to the precision of the calculated coefficients, the accuracy suffering accordingly. In the following section, a blockwise cubic spline method is employed to overcome this problem.

3.5.3. *Blockwise cubic spline interpolation*

A more sophisticated method of cubic interpolation considers a larger block of raw data and fits a series of cubic splines to it [12]. Interpolation points within that data block can then be found without having to recalculate the splines. This method generally produces better results than the piecewise cubic approach since the first and second derivatives of the interpolated curve are continuous, producing a smooth curve through all data points. As illustrated in Fig. 11, the cubic spline interpolation curve follows the actual signal very closely. Figures 12 and 13 show the spectra obtained by this cubic spline method. The noise floor for both speeds is greatly reduced over that of the previously discussed methods. An additional bonus of this method is that quick, single precision calculations are sufficient to ensure adequate accuracy.

3.5.4. *Interpolation summary*

All previously discussed interpolation techniques generated interpolation curves different from the input test sinusoid. This is expected because the original function is a sinusoidal and not a polynomial function. This analysis has shown that the higher-order polynomials produce more accurate results. Of the two cubic methods, block cubic is more accurate than piecewise cubic because the former generates a smoother curve with reduced sensitivity to precision in calculation. It was observed that each improvement in the interpolation procedure from linear, to cubic to spline reduced the noise floor in the resulting spectra by approximately an order of magnitude.

3.6. CONSIDERATIONS REGARDING NOISE

There are numerous possible sources of noise that can be divided into two broad categories: external and internal. External noise can come from stray electrical sources, poor ground connections, faulty transducer mounting, bad calibration and analog to digital quantisation. These external noise factors are no different than for classical fixed frequency analysis and therefore need not be considered here. Internal noise results from round-off error in calculations due to the available precision of variables, and approximations inherent in the chosen interpolation procedures. The internal sources of noise result from the computational and analysis methods and must be treated by the designer. The results from this study suggest that, given enough processing power, computed order tracking can virtually eliminate all internal noise.

3.7. EFFECTS OF DATA BLOCK SIZE

The vast majority of FFT routines require a specific number of input data points, usually, these quantities are of length 2^N (i.e. 256, 512, 1024, . . .). Highly efficient FFT routines can be written for data block sizes which have this property because of inherent symmetries in the FFT method [10]. The number of data points used depends on the results required. Increasing the number of data points results in a higher frequency resolution; it also increases calculation time (as in fixed frequency analysis). Although a high frequency resolution is desirable, a long calculation time is unacceptable for real-time implementation of the method. When using order tracking analysis, however, another consideration comes into play. Sampling for order tracking requires that a fixed number of data points be taken per revolution (this study used 12 resample points per revolution). Thus, for a larger data block, more shaft revolutions are required. In a run-up, the machine speed increases during the sampling process. If a large data block size is chosen, the method will have to wait through more shaft revolutions, and the data at the end of the block may be taken at a considerably higher speed than the first data points. The resulting spectrum may not be truly representative of the vibrations at the trigger speed. For example, a spectrum labelled 100 rpm, but containing data sampled from 100 to 250 rpm, may not be an accurate representation of the vibration frequenies and amplitudes at 100 rpm. It is also possible that the next trigger speed may be passed before enough data have been acquired for the last one.

4. SUMMARY AND CONCLUSIONS

Computed order tracking has recently been introduced to aid in the vibration analysis of rotating machinery. This procedure requires simpler and lower cost equipment than that associated with one traditional analog procedure. This new computational approach has not been previously examined to determine which inherent factors and assumptions have the greatest effect on accuracy. This study was executed to examine these issues, using a digital simulation that includes modeling the rotating machine, transducers, hardware and processing algorithm. Simulation prevented any external effects from influencing the tests, as would be expected with a physical apparatus. In addition, this permitted the determination of exact results, which were used as a base for comparison.

In all tests, the use of higher sampling rates on keyphasor and data signals resulted in improved accuracy. With raw data points closer together, the amplitude of the interpolated data is more accurate. Recognising that an excessive sample rate wastes computer resources by storing large quantities of raw data, it is important that a compromise be found that stikes a balance between data storage demands and accuracy.

The results presented in this paper show that the single greatest increase in spectral accuracy results from improvements of measuring the keyphasor pulse arrival time. If a data acquisition system is used which requires that both keyphasor and transducer channels use the same sample rate, then a sampling rate which produces good keyphasor timing accuracy should be chosen, as long as it is above the Nyquist limit for the transducer signal. This may require that much more transducer data be taken than is needed to ensure good keyphasor pulse timings. Use of higher-order interpolation also improved accuracy. Implementing a block cubic spline interpolation instead of a linear interpolation reduced background noise by almost two orders of magnitude.

For the simulation presented, more attention was paid to faithful modeling of the methods than to computational speed or efficiency. To move from testing by simulation to testing actual machines would require implementing the findings of this study and

optimising the computational techniques. If fast computing hardware is available, using digital signal processors or the like, a real-time implementation could be developed and tested.

ACKNOWLEDGMENT

The authors would like to acknowledge the Natural Sciences and Engineering Research Council of Canada for the partial financial support of this work.

REFERENCES

1. J. Berry 1991 How to track rolling element bearing health with vibration signature analysis *Sound and Vibration* **25**, 24–35.
2. J. I. Taylor 1994 *The Vibration Analysis Handbook* Tampa, Fl., Vibration Consultants, Inc.
3. Hewlett-Packard Company Hewlett-Packard Application Note 243-1, *Dynamic Signal Analyzer Applications*.
4. W. Potter 1990 *Tracking and Resampling Method and Apparatus for Monitoring the Performance of Rotating Machines*, United States Patent #4,912,661.
5. R. Potter 1990 *Sound and Vibration* **24**, 30–34 A new order tracking method for rotating machinery.
6. R. Potter and M. Gribler 1989 *SAE Noise and Vibration Conference*. 63–67. Computed order tracking obsoletes older methods.
7. C. N. Tan and J. Mathew 1990 *The Institution of Engineers Australia*, *Vibration and Noise Conference*, *Melbourne* 161–165, Monitoring the vibrations of variable and varying speed gearboxes.
8. Anonymous 1991 *Bentley Book One*, Minden, Nevada: Bentley Nevada Corporation.
9. W. H. Press, B. P. Flannery, S. A. Teukolsky and W. T. Vetterling 1989 *Numerical Recipes in C*. Cambridge: University of Cambridge Press.
10. E. O. Brigham 1974 *The Fast Fourier Transform*. Englewood Cliffs, NJ: Prentice-Hall.
11. E. D. S. Munck 1994 Computed Order Tracking Applied to Vibration Analysis of Rotating Machinery. M.Sc. thesis, Department of Mechanical Engineering, University of Alberta, Edmonton, Alberta, Canada.
12. S. C. Chapra and R. P. Canale *Numerial Methods for Engineers*, 2nd. Edn. New York: McGraw-Hill.

APPENDIX A

To illustrate the concept of sampling time determination, consider the following example. Suppose that a single keyphasor has been placed on a shaft. This corresponds to $\Delta\Phi = 2\pi$. Now assume that a constant sampling interval of Δt has been used for the original raw data. Suppose that the keyphasor pulses have been detected on the discrete sample points 1, 5 and 11. According to the definitions in Section 1.2, this implies that $t_1 = 1\Delta t$; $t_2 = 5\Delta t$ and $t_3 = 11\Delta t$. The amplitude of the original signal, the sampled data points and the keyphasor arrival times are indicated in Fig. A1.

Substituting the indicated values of t_1, t_2, t_3 and $\Delta\Phi$ into equation (3) and solving yields,

$$\{b\} = \begin{Bmatrix} -1.8326 \\ 1.8850 \\ -0.0524 \end{Bmatrix}$$

It is desired to resample the raw constant Δt data at a constant $\Delta\theta$ intervals. Suppose that the desired shaft increment angle for resampling is $\Delta\theta = \pi/3$ (i.e. six samples per shaft revolution). Therefore the shaft angle, θ can be calculated at values of $\theta = k\Delta\theta$. To avoid

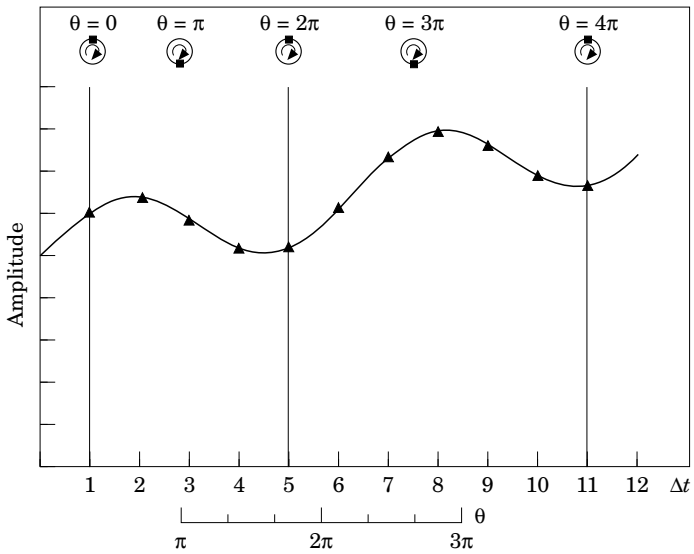

Figure A1. Uniform Δt sampling of a vibration signal; also shown are keyphasor arrival times.

overlap of the resampling regions, from one keyphasor pulse to the next, the admissible range of k, determined from equation (7), is $3 \leqslant k < 9$. The resampling times can now be calculated from equation (8). The following table shows the values of k, the corresponding values of θ and the calculated interpolation times, t.

The approximate locations of these resample times are placed on a second axis below the Δt axis in Fig. A1 for comparison. It is seen that they fall into the expected centre region of the three keyphasor arrival times.

The function was originally sampled at the constant Δt intervals and it is now desired to determine the corresponding amplitude values at the indicated constant $\Delta\theta$ intervals. This is known as the interpolation process. This procedure is graphically illustrated in Fig. A2. The first thing to note in this figure is that θ is now used as the primary abscissa and Δt as the secondary abscissa. The amplitude of the function is known at the constant Δt intervals and is shown by the filled triangular data points. It is now sought to determine what the amplitudes of the function are at the values of $\theta = \pi, 4\pi/3, 5\pi/3, \ldots$. Consider the first unknown resample point at $\theta = \pi$, for example, it is seen that it is enclosed by the known values of the function at $t = 2\Delta t$ and $t = 3\Delta t$. It is now just a simple matter to interpolate the value of the function between these two known points. To perform this, however, it is required to know the corresponding values of θ at the given points in time.

TABLE A1

Values of θ and t for $3 \leqslant k < 9$

k	θ	t
3	π	2.86725
4	$4\pi/3$	3.54317
5	$5\pi/3$	4.25227
6	2π	5
7	$7\pi/3$	5.79344
8	$8\pi/3$	6.64218

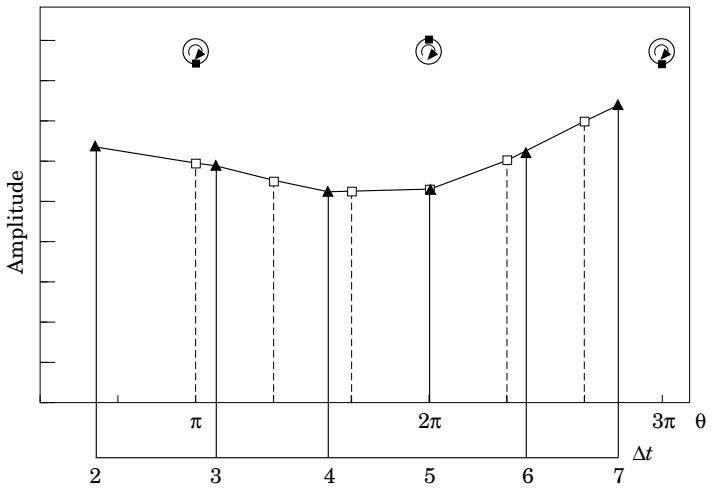

Figure A2. Resampling of vibration signal at a uniform $\Delta\theta$.

This is determined from equation (1), using the known $\{b_i\}$ values. In this example, a time of $t = 2\Delta t$ corresponds to $\theta = 1.7279$, while a time of $t = 3\Delta t$ corresponds to $\theta = 3.3510$. Now that these locations are known, any number of interpolation schemes may be used (as are described in Section 3.5). In Fig. A2, a trival linear interpolation method has been applied. The resulting resampled amplitudes are shown in hollow square markers.

The resampling and interpolation procedures are now complete. Once the desired number of resampled amplitudes have been computed, the data may be windowed and transformed to the order domain in the usual manner.

APPENDIX B

In this computed order tracking analysis, it is assumed that the shaft acceleration, α, is constant; i.e. $\alpha = \bar{\alpha}$. A constant shaft acceleration yields a linear relationship for the shaft speed, ω; i.e. $\omega = \bar{\alpha}t + \omega_0$. Assuming that the shaft starts from rest, then $\omega_0 = 0$. Therefore, the shaft speed is given by:

$$\omega = \bar{\alpha}t \tag{B1}$$

The shaft angle, θ, can then be determined from, $\theta = \bar{\alpha}t^2/2 + \theta_0$. For the purpose of this example, assume that the shaft angle starts from zero, therefore, $\theta_0 = 0$. This leaves,

$$\theta = \frac{\bar{\alpha}t^2}{2} \tag{B2}$$

It is of interest to determine the final shaft speed at the end of the any particular data collection period. Let the initial trigger shaft speed be ω_i. Substituting this speed into equation (B1) and solving for t, yields a staring time for this data collection period of $t_i = \omega_i/\bar{\alpha}$. Now substitute this time into equation (B2), this yields a starting angle of $\theta_i = \omega_i^2/(2\bar{\alpha})$. This is the starting angle for this period of data collection. Using a resampled blocksize of N and M resamples per shaft revolution, a total N/M shaft revolutions are required to collect the desired number of raw data points to be later resampled. If this number is added to the starting shaft angle θ_i, the final shaft angle is θ_f:

$$\theta_f = \theta_i + \frac{N}{M} = \frac{\omega_i^2}{2\bar{\alpha}} + \frac{N}{M} \tag{B3}$$

If the angle is substituted into equation (B2), the ending time, $t_f = \sqrt{2\theta_f/\bar{\alpha}}$, is found. Finally, this time is substituted into equation (B1), yielding the final shaft speed at the end of the data collection period

$$\omega_f = \bar{\alpha}\sqrt{\frac{2\theta_f}{\bar{\alpha}}} = \sqrt{2\bar{\alpha}\theta_f} = \sqrt{2\bar{\alpha}\left(\frac{\omega_i^2}{2\bar{\alpha}} + \frac{N}{M}\right)} = \sqrt{\left(\omega_i^2 + 2\bar{\alpha}\,\frac{N}{M}\right)}. \tag{B4}$$

As an example, in this analysis, $\bar{\alpha} = 10$ rpm/s $= 0.1667$ rev/s^2, $N = 512$, $M = 12$. Using a starting frequency of $\omega_i = 600$ rpm $= 10$ rev/s, this yields $\omega_f = 10.69$ rev/s $= 641.25$ rpm.